

Acoustic wave transmission through a bull's eye structure

Jun Mei,^{1,2} Bo Hou,¹ Manzhu Ke,² Shasha Peng,² Han Jia,² Zhengyou Liu,² Jing Shi,² Weijia Wen,^{1,a)} and Ping Sheng¹

¹Department of Physics, Hong Kong University of Science and Technology, Clear Water Bay, Kowloon, Hong Kong

²Department of Physics, Wuhan University, Wuhan 430072, China

(Received 13 February 2008; accepted 8 March 2008; published online 26 March 2008)

We study experimentally and theoretically acoustic transmission through a bull's eye structure, consisting of a central hole with concentric grooves imprinted on both sides of a thin brass plate. At wavelength slightly larger than the groove periodicity, a transmission peak was observed for normally incident acoustic wave, with excellent collimation (only $\pm 2^\circ$ divergence) at far field. This phenomenon is a manifestation of the two-dimensional circular version of structure-factor induced resonant transmission. Theoretical predictions based on this mechanism are in good agreement with the experiments. © 2008 American Institute of Physics. [DOI: 10.1063/1.2903704]

Soon after the discovery of extraordinary optical transmission through a metallic film with two-dimensional array of subwavelength holes,¹ it was found that there can be enhanced and collimated transmission through a single subwavelength hole surrounded by finite periodic rings of indentations (denoted as bull's eye).² The excitation of surface plasmons on metallic surfaces was believed to play a central role in the observed enhanced transmission phenomena; but there was a debate on the relative contribution of surface wave versus the diffraction mechanism.^{3–12} More recently, the interesting behavior of acoustic waves through a slit, surrounded by a one-dimensional (1D) finite array of grooves, was investigated theoretically with the conclusion that acoustic surface waves were mainly responsible for the enhanced transmission and collimation.¹³ Extraordinary acoustic wave transmission through a 1D grating with very narrow apertures was also reported, and the coupling between the diffractive wave and waveguide mode was discovered to play an important role.¹⁴ Another systematic study of acoustic wave transmission through a two-dimensional (2D) periodic array of subwavelength holes in a brass plate has found a unified type of excitations that correspond to Fabry–Pérot resonances when the plate is thick, and which merge into the diffractive structure-factor induced excitations when the plate is thin.¹⁵ Between the two limits, the Fabry–Pérot resonance conditions were found to be tunable via diffractive evanescent waves.

It is the purpose of this study to examine the interaction of ultrasonic waves with a bull's eye structure. We show through detailed experimental and theoretical investigations that coherent diffraction is responsible for the observed enhanced transmission and collimation phenomena.

The bull's eye structure, shown in the inset of Fig. 1, was fabricated by patterning both sides of a thin brass plate with concentric periodic grooves around a single cylindrical hole. The thickness of the brass plate is 1.6 mm, and the diameter of the central hole is 0.5 mm. The groove period is 2.0 mm, and there are a total of 15 grooves. The width and depth of each groove are 0.5 and 0.3 mm, respectively.

To perform the ultrasonic transmittance measurements, the patterned sample was placed in a water tank, sandwiched between two immersion transducers employed as generator and receiver, respectively. We measured the far-field transmittance of ultrasonic waves at normal incidence. As a reference, the transmittance through a smooth brass plate (1.6 mm thick) with a single 0.5 mm diameter hole was also measured. In addition, we have carried out near-field and far-field scanings to verify the physical mechanism involved in the transmission process. A pinducer (1.5 mm in diameter) was mounted on a 2D translation stage and brought to a distance z (~ 0.1 wavelength for the near field and 15 wavelengths for the far field) from the transmission side of the sample surface to measure the pressure field distribution. Scanning was done along the x - y plane parallel to the brass plate surface, with a spatial resolution of 0.2×0.2 mm².

In Fig. 1, we show the measured amplitude transmittances as a function of frequency for both the bull's eye structure and the reference sample. It can be seen that there is a transmission peak at 0.71 MHz for bull's eye structure,

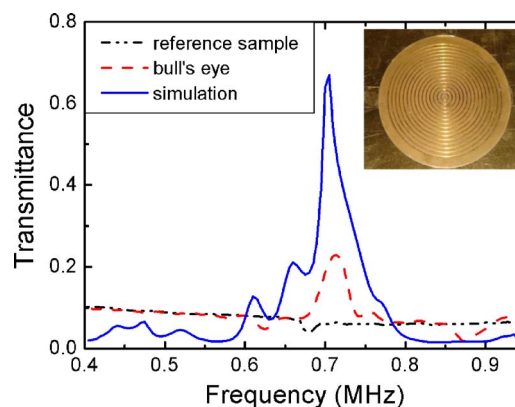


FIG. 1. (Color online) Measured amplitude transmittances plotted as a function of frequency for both the bull's eye structure and the reference sample, together with calculated power transmittance for bull's eye by using COMSOL MULTIPHYSICS. The inset shows an image of the sample, fabricated by patterning both sides of a thin brass plate with concentric periodic grooves around a single cylindrical hole. The thickness of the brass plate is 1.6 mm, and the diameter of the central hole is 0.5 mm. The groove period is 2.0 mm, and the groove width and depth are 0.5 and 0.3 mm, respectively.

^{a)} Author to whom correspondence should be addressed. Electronic mail: phwen@ust.hk.

while such peak is missing for the reference sample. In Fig. 1, we also plot the power transmittance calculated by using COMSOL MULTIPHYSICS,¹⁶ a finite-element solver used to simulate the pressure field distribution of acoustic waves passing through the bull's eye structure, both in the near field and in the far field. It can be seen from Fig. 1 that the predicted peak position agrees well with the experimental data (as well as the collimated nature of the transmitted beam, see below). However, the measured transmittance is much lower than that predicted; the precise reason for this disagreement is yet to be uncovered.

For ultrasonic waves in water, wavelength corresponding to 0.71 MHz is 2.1 mm, which is slightly larger than the groove period of bull's eye, i.e., 2.0 mm. This close correspondence is a strong clue indicating the enhanced transmittance to arise from the diffraction effect. It has been shown that enhanced acoustic wave transmission through hole arrays in perfectly rigid thin plate, where there can be no surface waves, may be related (via Babinet's principle) to "resonant" reflection by its complementary structure, i.e., planar arrays of perfectly rigid disks.¹⁵ In fact, both were associated with the *divergence* in the scattering structure factor, owing to the coherent addition of the Bragg scattering amplitudes.

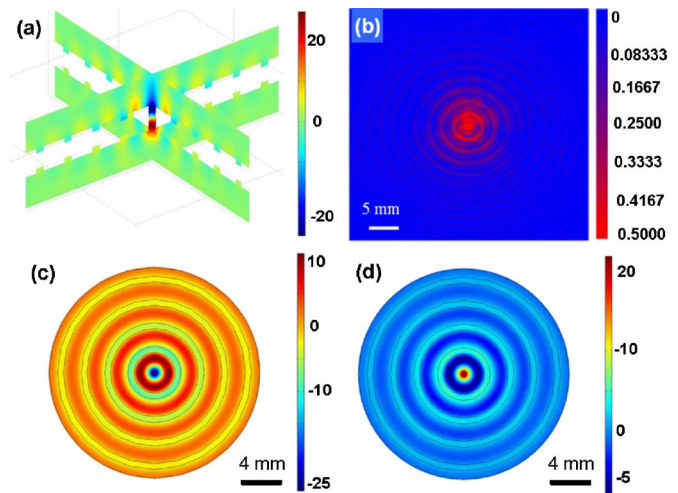


FIG. 2. (Color online) (a) Calculated near-field pressure field amplitude at the resonant transmission frequency of 0.71 MHz, plotted in three-dimensional. The node at the middle of the hole is evident. (b) Scanned near-field (at $\sim 1/10$ wavelength from the transmission side of the plate surface) pressure amplitude (absolute value) distribution for an area of $40 \times 40 \text{ mm}^2$ at the same resonant frequency. [(c) and (d)] Calculated near-field pressure amplitude distribution on the incident and the transmission sides of the brass plate, respectively, at the same resonant frequency.

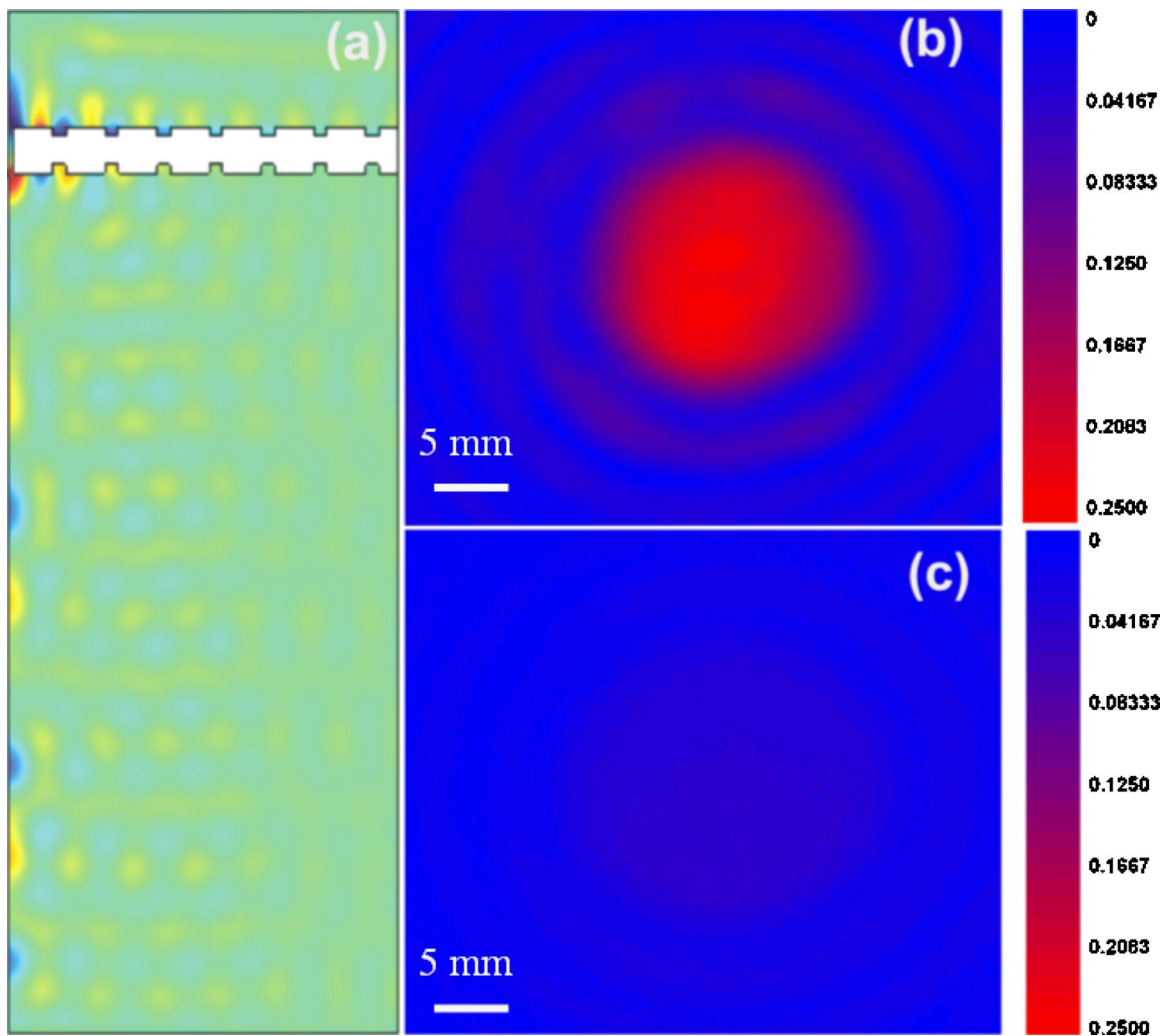


FIG. 3. (Color online) (a) Calculated far-field pressure amplitude distribution at 0.71 MHz. (b) Experimentally scanned far-field (~ 15 wavelengths from the transmission side of the plate surface) pressure amplitude (absolute value) distributions for an area of $40 \times 40 \text{ mm}^2$, for the bull's eye structure at 0.71 MHz. (c) Same as (b), for the reference sample.

As a result, a quasisurface mode with frequency close to the onset of the first diffraction order (wavelength λ slightly larger than the lattice constant a) always exists,¹⁵ denoted “structure-factor-induced surface modes,” or SF resonances. We expect the same mechanism to also apply to bull’s eye structure, which may be viewed as having 1D periodicity along the radial direction.

To be more specific, consider the complementary structure to the bull’s eye—a planar array of thin, concentric rings. It is well known that 2D functions with axial symmetry can be Fourier transformed by using the zeroth order Bessel function:

$$\begin{aligned} \int_{-\infty}^{\infty} \int_{-\infty}^{\infty} f(x,y) e^{i\vec{k}\cdot\vec{r}} dx dy &= \int_0^{\infty} \int_0^{2\pi} f(\rho, \theta) e^{i\vec{k}\cdot\vec{\rho}} \rho d\rho d\theta \\ &= 2\pi \int_0^{\infty} f(\rho) J_0(k\rho) \rho d\rho. \end{aligned} \quad (1)$$

In Eq. (1), the k is understood to be in the plane, i.e., k_{\parallel} . It follows that when a plane wave $\exp[i(\omega/c)z]$ is incident on the concentric rings, the reflection from each ring is proportional to $J_0(k\rho) \exp(-i\sqrt{(\omega/c)^2 - k_{\parallel}^2}z) \rho d\rho$, with a factor $g(\omega)$ to account for the relative phase difference between the rings. As a result, the total reflected wave from all the concentric rings can be written as $\int g(\omega) J_0(k_{\parallel}\rho) \times \exp(-i\sqrt{(\omega/c)^2 - k_{\parallel}^2}z) \rho d\rho$. At the resonant wavelength, when all the rings reflect the incident plane wave coherently, the far-field reflection amplitude (not including the incident plane wave) should be at its maximum—i.e., the phase difference between two nearest-neighbor rings should be a multiple of 2π , or $k_{\parallel}a = n2\pi$, a being the ring periodicity. Hence, we should have $k_{\parallel} = 2\pi/a$ for the lowest frequency resonance. For reflection, $(\omega/c)^2$ should be slightly larger than $k_{\parallel}^2 = (2\pi/a)^2$ in order to have a nonevanescing wave. It follows that the longest resonant wavelength should be slightly larger than the periodicity of the concentric rings.

It follows from Babinet’s principle that bull’s eye structure should have maximum transmission at the same wavelength, i.e., at a wavelength slightly larger than the period of grooves. In fact, the above analysis is supported by the pressure field distribution in our simulations. As shown clearly in Fig. 2, on both sides of the thin brass plate, there is a trough-crest type of oscillations within one wavelength.

COMSOL MULTIPHYSICS was used to obtain quantitative predictions. Calculated near-field pressure amplitude distributions at 0.71 MHz are plotted in Figs. 2(a), 2(c), and 2(d). Several interesting points should be noted. First, it can be seen that the wave amplitude is very strong at both the incident and transmission sides of the central hole, reaching about 28 times the incident wave amplitude. Second, the pressure field on the transmission side of the brass plate is noted to be out of phase from that of the incident side. Third, along the propagation direction (z), there is a node in the middle of the central hole, part of a standing-wave-like field distribution which looks very like a Fabry–Pérot (FP) resonance along the z direction [see Fig. 2(a)]. In conjunction with the z variation of the central hole, the simulated near-field amplitudes on both sides of the sample display peak to trough oscillations, with a separation that is very close to

1 mm far away from the central hole, but larger than 1 mm close to the central hole. This can be seen by careful examination of Figs. 2(c) and 2(d). This latter deviation (from 1 mm) can be understood as an effect of the FP resonance in the central hole. It is well known that the FP resonant condition can be expressed as $t = n\lambda/2$, where t is the path length. By writing $(\omega/c)^2 = k_{\perp}^2 + k_{\parallel}^2$ and specifying $k_{\perp} = 1.96 \text{ mm}^{-1}$ to satisfy the FP condition $t = \pi/k_{\perp}$ for the thickness t of the brass plate, we obtain $k_{\parallel} = \sqrt{(\omega/c)^2 - k_{\perp}^2} = 2.26 \text{ mm}^{-1}$, implying a peak-trough distance of $\lambda_{\parallel}/2 = \pi/k_{\parallel} = 1.39 \text{ mm}$. This is nearly what is obtained from simulation close to the central hole, displayed in Figs. 2(a), 2(c), and 2(d). We also plot the experimental results for near-field scanning data in Fig. 2(b). It is seen that the qualitative agreement between theory and experiment is very good.

The collimation effect is very striking. As shown in Fig. 3(a), the far-field acoustic wave on the transmission side is also in the form of a tight beam with a lateral dimension not exceeding the groove periodicity. The full width at half maximum divergence is $\pm 2^\circ$. As analyzed above, it is the coherent scattering which leads to the emergence of a strongly collimated beam in the far-field region. In Figs. 3(b) and 3(c), we also plot the scanned results at a distance of about 15 wavelengths from the transmission side of the surface, for both the bull’s eye structure [Fig. 3(b)] and the reference sample [Fig. 3(c)]. Compared to the reference sample, the collimation effect for bull’s eye structure is very evident.

Due to the enhanced and collimated transmission effects, the bull’s eye structure is expected to find applications as a component of integrated transducer in acoustic focusing devices and ultrasonic detection devices.

The authors would like to acknowledge the support by NSFC/RGC joint research Grant Nos. N_HKUST632/07 and 10731160613.

¹T. W. Ebbesen, H. J. Lezec, H. F. Ghaemi, T. Thio, and P. A. Wolff, *Nature (London)* **391**, 667 (1998).

²H. J. Lezec, A. Degiron, E. Devaux, R. A. Linke, L. Martin-Moreno, F. J. García-Vidal, and T. W. Ebbesen, *Science* **297**, 820 (2002).

³M. M. J. Treacy, *Phys. Rev. B* **66**, 195105 (2002).

⁴H. J. Lezec and T. Thio, *Opt. Express* **12**, 3629 (2004).

⁵J. A. Porto, F. J. García-Vidal, and J. B. Pendry, *Phys. Rev. Lett.* **83**, 2845 (1999).

⁶H. E. Went, A. P. Hibbins, J. R. Sambles, C. R. Lawrence, and A. P. Crick, *Appl. Phys. Lett.* **77**, 2789 (2000).

⁷Y. Takakura, *Phys. Rev. Lett.* **86**, 5601 (2001).

⁸F. Yang and J. R. Sambles, *Phys. Rev. Lett.* **89**, 063901 (2002).

⁹D. C. Skigin and R. A. Depine, *Phys. Rev. Lett.* **95**, 217402 (2005).

¹⁰S. Selcuk, K. Woo, D. B. Tanner, A. F. Hebard, A. G. Borisov, and S. V. Shabanov, *Phys. Rev. Lett.* **97**, 067403 (2006).

¹¹F. J. García de Abajo, R. Gómez-Medina, and J. J. Sáenz, *Phys. Rev. E* **72**, 016608 (2005).

¹²F. J. García de Abajo and J. J. Sáenz, *Phys. Rev. Lett.* **95**, 233901 (2005).

¹³J. Christensen, A. I. Fernández-Domínguez, F. de Leon-Pérez, L. Martín-Moreno, and F. J. García-Vidal, *Nat. Phys.* **3**, 851 (2007).

¹⁴M. H. Lu, X.-K. Liu, L. Feng, J. Li, C.-P. Huang, Y.-F. Chen, Y.-Y. Zhu, S.-N. Zhu, and N.-B. Ming, *Phys. Rev. Lett.* **99**, 174301 (2007).

¹⁵B. Hou, J. Mei, M. Ke, W. Wen, Z. Y. Liu, J. Shi, and P. Sheng, *Phys. Rev. B* **76**, 054303 (2007).

¹⁶COMSOL MULTIPHYSICS, version 3.4. COMSOL MULTIPHYSICS (formerly known as FEMLAB) is a finite element analysis/solver software package for physics and engineering applications.